

Relativistic Rotating Vector Model

Maxim Lyutikov

Department of Physics, Purdue University, 525 Northwestern Avenue, West Lafayette, IN 47907-2036, USA; lyutikov@purdue.edu

Received/Accepted

ABSTRACT

The direction of polarization produced by a moving source rotates with the respect to the rest frame. We show that this effect, induced by pulsar rotation, leads to an important correction to polarization swings within the framework of rotating vector model (RVM). We construct relativistic RVM taking into account finite heights of the emission region that lead to aberration, time-of-travel effects and relativistic rotation of polarization. Polarizations swings at different frequencies can be used, within the assumption of the radius-to-frequency mapping, to infer emission radii and geometry of pulsars.

1. Classic Rotating Vector Model

The Rotating Vector Model, RVM, Radhakrishnan & Cooke (1969) is a cornerstone of pulsar theory. It explains, at least qualitatively, polarization swings observed in many pulsars (*e.g.*, Manchester et al. 1975). But often observations show deviation from model (Edwards & Stappers 2004). A number of attempts have been made to improve the model either considering finite emission heights (Blaskiewicz et al. 1991, *e.g.*,) or distortions of the magnetosphere (*e.g.*, Hibschan & Arons 2001; Craig & Romani 2012). Another important effect is the rotation of the polarization direction due to the relativistic motion of the emitter (Cocke & Holm 1972; Ferguson 1973; Blandford & Königl 1979; Lyutikov et al. 2003, 2005; Viironen & Poutanen 2004).

Mathematical relations are best solved in a rest frame of the pulsar. In this frame the magnetic moment is directed along z axis, so that a unit μ -vector is $\mu = \{0, 0, 1\}$. For a unit radius vector $\hat{\mathbf{r}} = \{\cos \phi \sin \theta, \sin \phi \sin \theta, \cos \theta\}$ the unit vector along the magnetic field at a point $\{\theta, \phi\}$ is

$$\mathbf{b} = \left\{ \frac{3\sqrt{2} \sin \theta \cos \theta \cos \phi}{\sqrt{3 \cos(2\theta) + 5}}, \frac{3\sqrt{2} \sin \theta \cos \theta \sin \phi}{\sqrt{3 \cos 2\theta + 5}}, \frac{3 \cos 2\theta + 1}{\sqrt{6 \cos 2\theta + 10}} \right\} \quad (1)$$

Introducing rotation L_t and inclination L_α operators,

$$L_t = \begin{pmatrix} \cos \Omega t & -\sin \Omega t & 0 \\ \sin \Omega t & \cos \Omega t & 0 \\ 0 & 0 & 1 \end{pmatrix}, L_\alpha = \begin{pmatrix} \cos \alpha & 0 & -\sin \alpha \\ 0 & 1 & 0 \\ \sin \alpha & 0 & \cos \alpha \end{pmatrix}, \quad (2)$$

the line of sight in that frame is

$$\mathbf{n} = L_\alpha \cdot L_t \cdot \mathbf{n}_0, \mathbf{n}_0 = \{\sin \theta_{ob}, 0, \cos \theta_{ob}\} \quad (3)$$

while the plane of the sky is determined by two vectors

$$\begin{aligned} \mathbf{l} &= L_t \cdot L_\alpha \cdot \mathbf{l}_0 \\ \mathbf{m} &= L_t \cdot L_\alpha \cdot \mathbf{m}_0 \\ \mathbf{l}_0 &= \{0, 1, 0\} \\ \mathbf{m}_0 &= \{\cos \theta_{ob}, 0, -\sin \theta_{ob}\} \end{aligned} \quad (4)$$

In the above relations α is the pulsar inclination angle (angle between rotation and magnetic axes), θ_{ob} is the viewing angle - (angle between rotation axis and the line of sight).

RVM assumes that emission is directed align the local magnetic field, thus the condition $\mathbf{b} \parallel \mathbf{n}$ determines the coordinates $\{\theta, \phi\}$ of a point in the magnetosphere that contributes to the emission. Conventionally (assuming that emission occurs at $r = 0$) the requirement $\mathbf{b} \parallel \mathbf{n}_0$ gives

$$\begin{aligned} \tan \phi &= \frac{\sin \theta_{ob} \sin \Omega t}{\cos \alpha \sin \theta_{ob} \cos \Omega t - \sin \alpha \cos \theta_{ob}} \\ \frac{3 \cos 2\theta + 1}{\sqrt{6 \cos 2\theta + 10}} &= \cos \alpha \cos \theta_{ob} + \sin \alpha \sin \theta_{ob} \cos \Omega t \end{aligned} \quad (5)$$

For given parameters of the pulsar and the LoS these two equations determine the emission point $\{\theta, \phi\}$ that contributes to the emission.

To find the polarization direction we note that within the RVM the polarization is perpendicular to the azimuthal vector

$$\mathbf{e}_\phi = \{-\sin \phi, \cos \phi, 0\} \quad (6)$$

and to the LoS \mathbf{n} . Thus polarization is along

$$\mathbf{e}_p = \mathbf{e}_\phi \times \mathbf{n} \quad (7)$$

(\mathbf{e}_p can be normalized, but the normalization factor cancels out if we calculate $\tan \chi$.) The polarization angle is

$$\tan \chi = \frac{\mathbf{e}_p \cdot \mathbf{l}}{\mathbf{e}_p \cdot \mathbf{m}} \quad (8)$$

evaluates to

$$\tan \chi = -\frac{\sin \alpha \sin \phi \sin \theta_{ob} + \cos \alpha \sin \phi \cos \theta_{ob} \cos \Omega t - \cos \phi \cos \theta_{ob} \sin \Omega t}{\cos \alpha \sin \phi \sin \Omega t + \cos \phi \cos \Omega t} \quad (9)$$

Using Eq. (5) to eliminate ϕ we find (Radhakrishnan & Cooke 1969)

$$\tan(\chi) = \frac{\sin \alpha \sin \Omega t}{\sin \alpha \cos \theta_{ob} \cos \Omega t - \cos \alpha \sin \theta_{ob}} \quad (10)$$

2. Relativistic effects

2.1. Aberration

Finite distance of the emission region from the center of the star introduces a number of corrections to the classic RVM. Some of these corrections - aberration - have been considered previously (*e.g.*, Blaskiewicz et al. 1991). Here we include another important relativistic effect: rotation of polarization produced by a moving source. (Below the radius r is normalized to the light cylinder radius r ; we use spherical system of coordinates, so $r = 1$ does not mean a point is located on the light cylinder; speed of light is set to unity).

In the chosen frame the angular and the linear velocities are

$$\begin{aligned} \boldsymbol{\Omega} &= L_t \cdot L_\alpha \cdot \boldsymbol{\Omega}_0 \\ \boldsymbol{\Omega}_0 &= \{0, 0, \Omega\} \\ v &= r\boldsymbol{\Omega} \times \hat{\mathbf{r}} \end{aligned} \quad (11)$$

The first relativistic effects is aberration: in the pulsar frame the wave is emitted along

$$\mathbf{n}_1 = \frac{\mathbf{n} - \mathbf{v}\gamma \left(1 - \frac{\gamma}{1+\gamma}(\mathbf{n} \cdot \mathbf{v})\right)}{\gamma(1 - (\mathbf{n} \cdot \mathbf{v}))} \quad (12)$$

The condition $\mathbf{n}_1 \parallel \mathbf{b}$ then determines θ and ϕ of the emission point. This condition is difficult to resolve analytically even for small r , so we resort to numerical methods, Fig. 1

2.2. Time-of-flight effects

Finite height of emission will also affect polarization sweeps due to time of travel effects. Let us calculate it with respect to the plane parallel to the plane of the sky and passing

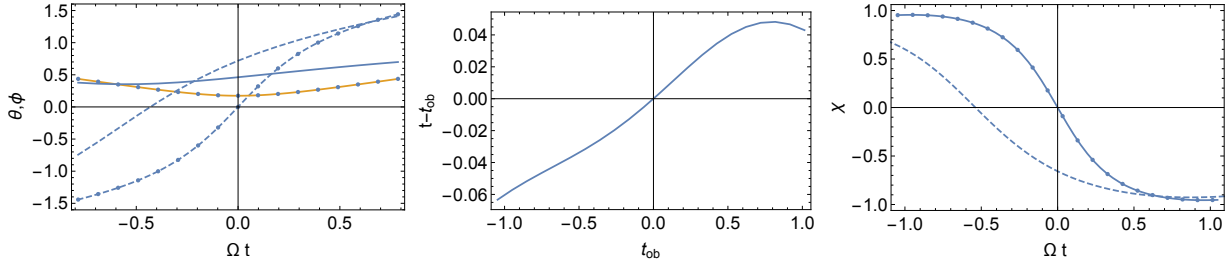


Fig. 1.— Various relativistic corrections for the case of inclination angle $\alpha = \pi/4$, viewing angle $\theta_{ob} = \pi/3$ distance to the star $r = 1$. *Left Panel:* Effects of aberration. Plotted are the location of the points in the magnetosphere contributing to emission. Solid lines are $\theta(t)$, dashed lines are $\phi(t)$. Lines with dots are the conventional RVM, dots are numerical results (agreement of numerical results with the analytic RVM also serves as a test of our numerical scheme). *Center Panel:* time-of-travel effects. Plotted is the difference between the coordinate and the observer time versus the observer time. We see that time-of-flight corrections are typically small for the parameters chosen. *Right Panel:* Classic RVM (solid line with dots corresponding to the numerical solutions of Eq. (10)) and the effects of relativistic rotation of polarization for emission height $r = 1$ (dashed line).

through the pulsar. The corresponding observer time is $t_{ob} = t - r(\hat{\mathbf{r}} \cdot \mathbf{n})$. For convenience we shift the observer times t_{ob} by t_0 so that $t = 0$ corresponds to $t_{ob} = 0$,

$$t_{ob} = t - r(\hat{\mathbf{r}} \cdot \mathbf{n}) + t_0 \quad (13)$$

For a given observer time t_{ob} we invert relation (13) to find the emission time t , see Fig. 1, Center Panel.

2.3. Rotation of polarization from moving source

Finally, the most important effect that has previously been missed is rotation polarization direction due to the motion of the source. This effect has previously been considered for the case of synchrotron emission by relativistically moving sources in AGNe Lyutikov et al. (2005) and GRBs Lyutikov et al. (2003). We can use the result of Lyutikov et al. (2003) with the following substitution. In case of synchrotron emission the direction of polarization *in the plasma rest frame* is orthogonal both to the direction of wave propagation and the projection of the magnetic field onto the plane orthogonal to the direction of propagation. In case of curvature emission (which is assumed as a basic emission mechanism for the rotating vector model) the direction of polarization in the pulsar frame is orthogonal to the photon

propagation and *the vector normal to the plane of the magnetic field* - for purely dipole field this is the azimuthal vector \mathbf{e}_ϕ , Eq. (6).

Thus, we can use the relativistic polarization transformation, Eq. (3) of Lyutikov et al. (2003), substituting $\mathbf{B}' \rightarrow \mathbf{e}_\phi$; we find

$$\begin{aligned} \mathbf{e}_p &= \frac{\mathbf{n} \times \mathbf{q}'}{\sqrt{q'^2 - (\mathbf{n} \cdot \mathbf{q}')^2}}, \\ \mathbf{q}' &= \mathbf{e}_\phi + \mathbf{n} \times (\mathbf{v} \times \mathbf{e}_\phi) - \frac{\gamma}{1 + \gamma} (\mathbf{e}_\phi \cdot \mathbf{v}) \mathbf{v}. \end{aligned} \quad (14)$$

Equation (14) also demonstrates that for the purely poloidal motion ($\mathbf{e}_\phi \cdot \mathbf{v} = 0$) along the emission direction does not affect the polarization - for $\mathbf{v} \parallel \mathbf{n}$ we have $\mathbf{q}' = \mathbf{e}_\phi$.

We have formally solved the relativistic polarization in the framework of the RVM: for a given direction to the observer frame, Eq. (3), Eq. (12) gives the direction in the rotating pulsar frame; it must be aligned with the local magnetic field Eq. (1). This condition gives two angular coordinates $\{\theta, \phi\}$ corresponding to the emission point. Next, Eq. (14) gives the direction of the polarization vector and Eq. (8) gives the polarization angle.

2.4. Putting it all together

Next we put all the relativistic effects together: aberration, time of flight, and rotation of polarization, Fig. 2.

A few examples of polarization swings for various parameters are given in Fig. 3

2.5. A simple example

The above relations are highly complicated and cannot be resolved analytically even in the limit of small emission radii. Let us illustrate the principle using an over-simplified example: an aligned rotator, $\alpha = 0$. The conventional RVM then simply gives, Eq. (5), $\chi = 0$ - polarization is aligned with the projection of the rotation axis onto the plane of the sky. Relations (5) give in this case

$$\begin{aligned} \tan \theta_{ob} &= \frac{3 \sin 2\theta}{3 \cos 2\theta + 1} \\ \phi &= \Omega t \end{aligned} \quad (15)$$

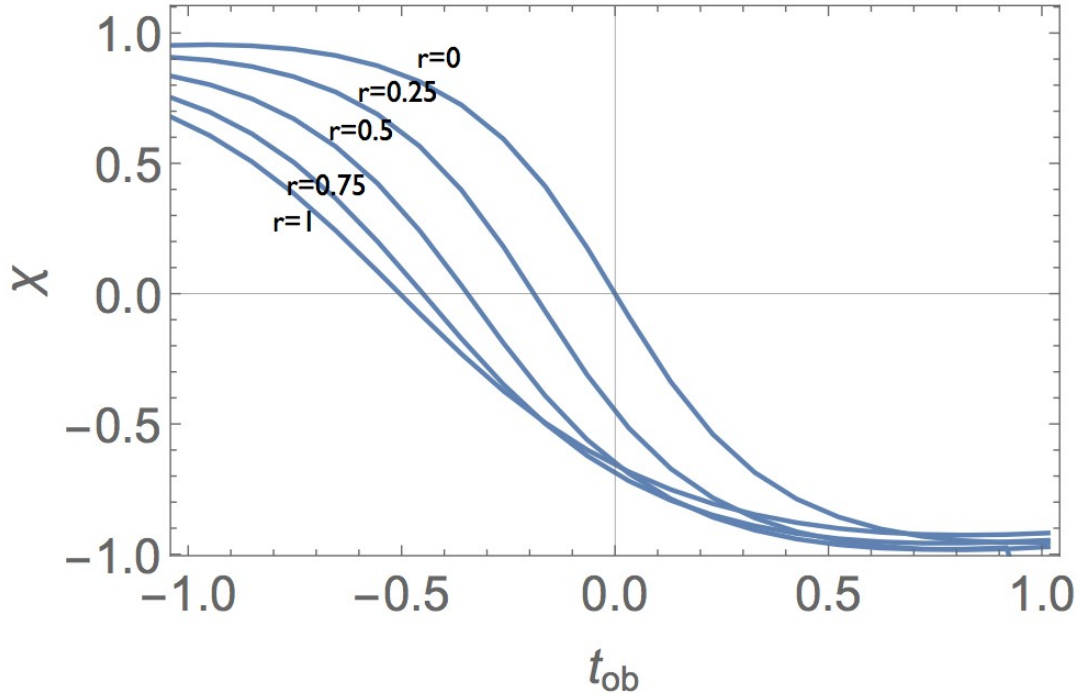


Fig. 2.— Polarization angle sweeps for different emission radii taking into account all the relativistic effects: aberration, time of flight and rotation of polarization. Distance is measured in the light cylinder radii. Inclination angle $\alpha = \pi/4$, viewing angle $\theta_{ob} = \pi/3$, $r = 1$.

For finite emission radii, taking into account aberration (in the limit $r \rightarrow 0$) gives

$$\phi = \Omega t - r\Omega \frac{\sin \theta}{\sin \theta_{ob}} \quad (16)$$

while relation between θ and θ_{ob} remains the same as (15).

The polarization angle becomes

$$\tan \chi \approx r\Omega \frac{\sin \theta}{\sin \theta_{ob}} = r\Omega \left(\cos \theta - \frac{\sec \theta}{3} \right) \approx \frac{r\Omega}{6}, \text{ for } \theta_{ob} \ll 1 \quad (17)$$

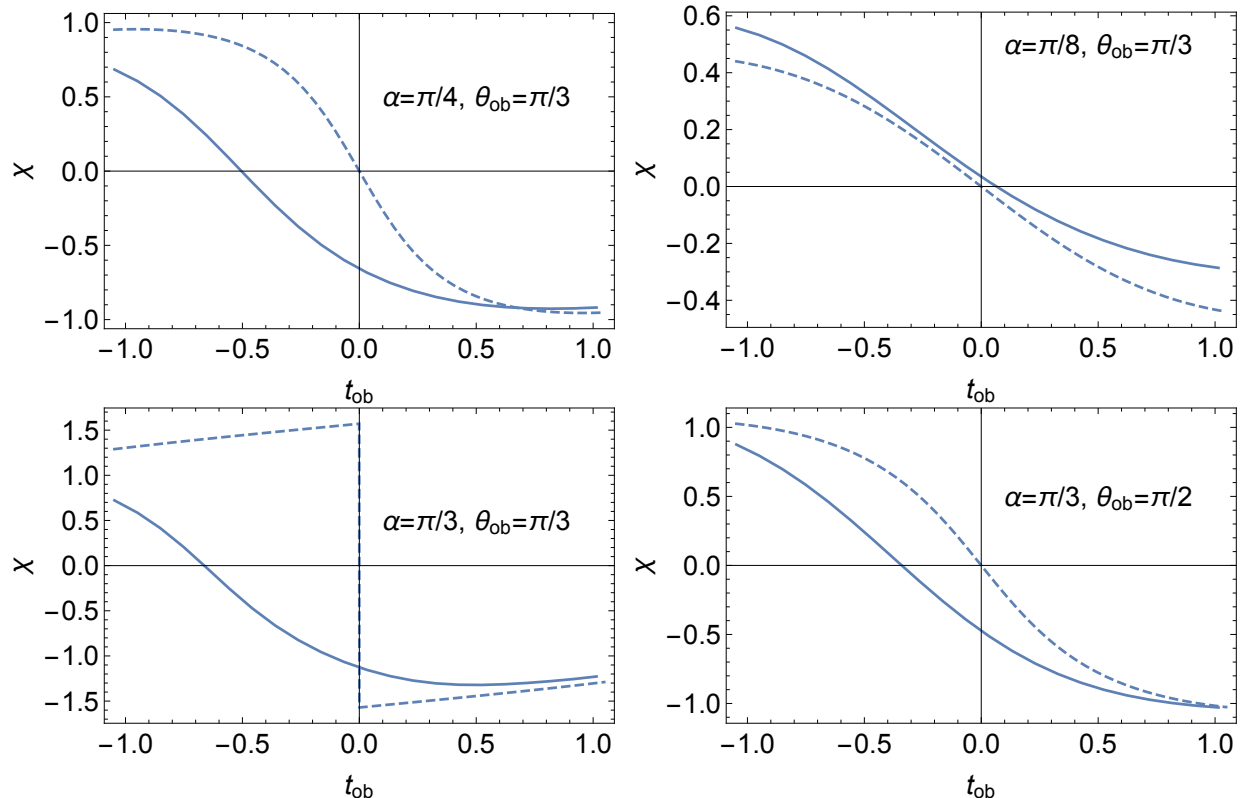


Fig. 3.— Polarization angle sweeps for different parameters; $r = 1$.

3. Discussion

The key point of the present paper is to point out that an important relativistic effects – rotation of the direction of polarization emitted by a moving source – has been previously missed in the modifications of RVM. The effect is linear in $r\Omega$, as well as aberrations and time of travel effects. As Fig. 2 demonstrates, the relativistic effects become important, somewhat unexpectedly, at fairly small radii, 25% – 50% of the light cylinder. These effects are bound to be dominant in millisecond pulsars. We foresee that these effects will also be important in modeling the light curves (and radio polarization swings) in the γ -ray pulsars (Abdo et al. 2013).

Fig. 2 also demonstrates that polarizations swings measured at different frequencies can constrain the radius-to-frequency mapping. Or inversely, polarizations swings at different frequencies can be used to infer the emission radius and the geometry of a particular pulsar. One of the major constraints is the assumption of the dipolar structure – at larger radii the sweep-back of the field lines and the distortion of the poloidal structure would become important. We leave these applications to a future work.

I would like to thank Carl Gwinn and Yuri Poutanen for discussions and Universitat Autònoma de Barcelona for hospitality.

REFERENCES

- Abdo, A. A., Ajello, M., Allafort, A., Baldini, L., Ballet, J., Barbiellini, G., Baring, M. G., Bastieri, D., Belfiore, A., Bellazzini, R., & et al. 2013, *ApJS*, 208, 17
- Blandford, R. D. & Königl, A. 1979, *ApJ*, 232, 34
- Blaskiewicz, M., Cordes, J. M., & Wasserman, I. 1991, *ApJ*, 370, 643
- Cocke, W. J. & Holm, D. A. 1972, *Nature Physical Science*, 240, 161
- Craig, H. A. & Romani, R. W. 2012, *ApJ*, 755, 137
- Edwards, R. T. & Stappers, B. W. 2004, *A&A*, 421, 681
- Ferguson, D. C. 1973, *ApJ*, 183, 977
- Hirschman, J. A. & Arons, J. 2001, *ApJ*, 546, 382
- Lyutikov, M., Pariev, V. I., & Blandford, R. D. 2003, *ApJ*, 597, 998
- Lyutikov, M., Pariev, V. I., & Gabuzda, D. C. 2005, *MNRAS*, 360, 869
- Manchester, R. N., Taylor, J. H., & Huguenin, G. R. 1975, *ApJ*, 196, 83
- Radhakrishnan, V. & Cooke, D. J. 1969, *Astrophys. Lett.*, 3, 225
- Viironen, K. & Poutanen, J. 2004, *A&A*, 426, 985